International Journal of Pattern Recognition
and Artificial Intelligence
Vol. 24, No. 4 (2010) 1–16

DOI: 10.1142/S021800141000807X

World Scientific
www.worldscientific.com

SKELETONIZATION WITH PARTICLE FILTERS

YUCHUN TANG
Research Center of Sectional and Imaging Anatomy
Shandong University School of Medicine
44#, Wenhua Xi Road, Jinan, Shandong 250012, China
yuchuntang@ucla.edu

XIANG BAI*
Department of Electronics and Information Engineering
Huazhong University of Science and Technology
NO. 1037, Luoyu Road, Wuhan, Hubei 430074, China
xbai@hust.edu.cn

XINGWEI YANG
Department of Computer and Information Sciences
Temple University
1805 North Broad Street, Philadelphia, PA 19122
xingwei.yang@temple.edu

LIANG LIN
Department of Statistics
University of California, Los Angeles
Los Angeles, CA 90095, US
linliang@ieee.org

SHUWEI LIU
Research Center of Sectional and Imaging Anatomy
Shandong University School of Medicine
44#, Wenhua Xi Road, Jinan, Shandong 250012, China
liusw@sdu.edu.cn

LONGIN JAN LATECKI
Department of Computer and Information Sciences
Temple University
1805 North Broad Street, Philadelphia, PA 19122
latecki@temple.edu

*Author for correspondence.

We present a novel method to obtain high quality skeletons of binary shapes. The obtained skeletons are connected and one pixel thick. They do not require any pruning or any other post-processing. The computation is composed of two major parts. First, a small set of salient contour points is computed. We use Discrete Curve Evolution, but any other robust method could be used. Second, particle filters are used to obtain the skeleton. The main idea is that the particles walk along the skeletal paths between pairs of the salient points. We provide experimental results that clearly demonstrate that the proposed method significantly outperforms other well-known methods for skeleton computation. Moreover, we propose an extension of our method to computing skeletons of gray level images and provide promising experimental results.

Keywords: Skeleton; skeletonization; skeletal path; particle filter.

1. Introduction

The skeleton is important for object representation and recognition in different areas, such as image retrieval and computer graphics, character recognition, image processing, and the analysis of biomedical images.[8] The skeleton is an abstraction of objects that at the same time contains both shape features and topological structures of the original object. Therefore, many researchers have worked on matching skeleton structures represented by graphs or trees.[3,5,27,30] However, as the skeleton is sensitive to the noise and deformation of the boundary, which may seriously disturb the topology of the skeleton graph, these methods cannot work on complex shapes or shapes with obvious noise.

We list now properties of the ideal skeleton.

(1) it should preserve the topology of the original object.
(2) it should be stable under deformations.
(3) it should be invariant under Euclidean transformations such as rotations and translations.
(4) the position of the skeleton should be accurate.
(5) it should be composed of 1D arcs (i.e. one-pixel wide in digital images).
(6) it should represent significant visual parts of objects.

Properties (4) and (5) mean that the skeleton should contain the centers of maximal disks, and nothing more than the centers of maximal disks. Many typical methods cannot guarantee the property (4), such as the methods using thinning[29] or Active Contour model.[21] Property (6) means that there should be skeleton branches in every significant object part and that there should be no spurious branches that do not correspond to any object parts (which are usually due to noise).

Since most of the existing skeleton computation methods are not able to produce skeletons that satisfy property 6, skeleton pruning is applied. Its goal is to remove spurious branches. Clearly, a pruned skeleton should still have properties (1)−(6).

Ogniewicz and Kübler[24] presented a few significant measures for pruning complex Voronoi skeletons without disconnecting the skeletons, but it may lead to topology violation. The method in Ref. 26 has difficulty in distinguishing noise from low frequency shape information on boundaries. The skeleton generated in Ref. 9 cannot

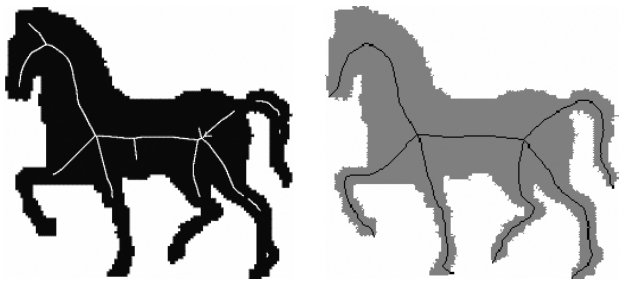

(a) (b)

Fig. 1. (a) Skeleton computed by the method in Ref. 8, (b) by the proposed method.

guarantee the property of the connectivity, as shown in the experimental results in Fig. 1(a). The skeleton computed by our method is shown in Fig. 1(b).

The method introduced by Bai *et al.*[4] can obtain excellent skeletons which contain most of the properties of ideal skeletons, but it cannot guarantee that the skeleton is one-pixel wide and it need the postprocessing. Compared to it, our method produces one-pixel thick skeletons without skeleton pruning.

Particle filters estimate the posterior probability density over the state space of a dynamic system. The key idea of this technique is to represent probability densities by sets of samples. By sampling in proportion to likelihood, particle filters focus the computational resources on regions with high likelihood, where good approximations are most important. Over the last few years, particle filters have been applied with great success to a variety of state estimation problems including visual tracking, speech recognition, mobile robot localization, robot map building, people tracking, and fault detection. Moreover, Adluru *et al.* have used particle filters in contour grouping.[1] The proposed method is the first one that utilizes particle filters in computing skeletons.

The proposed method first utilizes the Discrete Curve Evolution (DCE)[16,17] to simplify the contour, and to obtain a small set of salient points as vertices of the simplified polygon, but other approaches which produce stable salient points could also be used. The basic idea of the DCE is simple. In every evolutional step of DCE, a pair of consecutive line segments s_1, s_2 is replaced by a single line segment joining the endpoints of $s_1 \cup s_2$. The order of the substitution is determined by the relevance measure K given by:

$$K(S_1, S_2) = \frac{\beta(S_1, S_2) l(S_1) l(S_2)}{l(S_1) l(S_2)} \tag{1}$$

where line segments s_1, s_2 are the polygon sides incident to a vertex v, $\beta(s_1, s_2)$ is the turn angle at the common vertex of segments s_1, s_2, l is the length function normalized by the total length of a polygonal curve C. The higher value of $K(s_1, s_2)$, the larger is the contribution of the arc $s_1 \cup s_2$ to the shape. During the evolution, we will first remove the arcs with the smallest contribution. In Fig. 2, we show some results

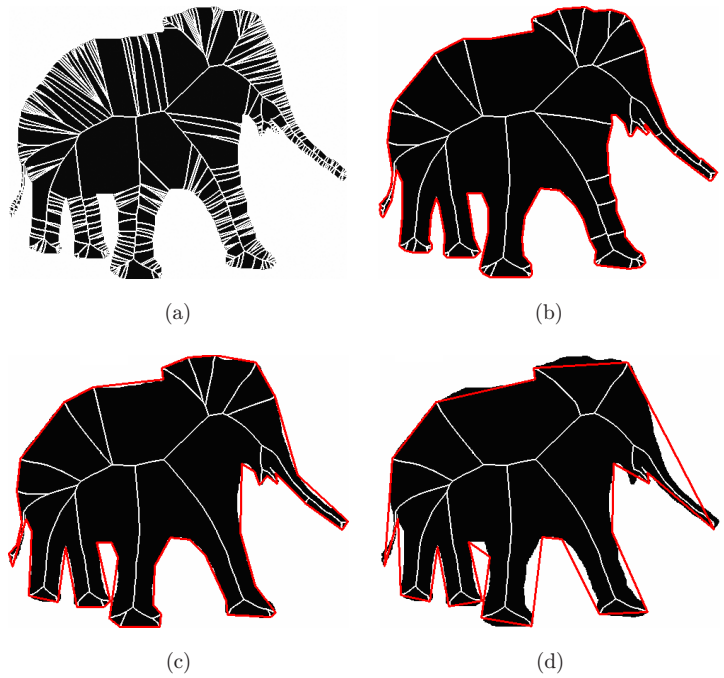

Fig. 2. Hierarchical skeleton of elephant obtained by pruning the input skeleton (left) with respect to contour segments obtained by the Discrete Curve Evolution (DCE). The outer (red) polylines show the corresponding DCE simplified contours.

to illustrate that each convex vertex of the DCE simplified polygon is guaranteed to be a skeleton endpoint.

We benefit from a geometric relation between the skeletal path and the contour, which is a key observation that motivates our approach: the endpoints of significant skeleton branches coincide with convex salient contour points. We illustrate the main ideas of the proposed method in Fig. 3. Let a and b be two salient contour points. They divide the contour into two parts $C = C_1 \cup C_2$ marked with red and blue colors, respectively. The skeleton path $p(a, b)$ from a to b is composed of centers of maximal disks that are tangent both to C_1 and to C_2. We use a particle filter to compute the path $p(a, b)$. The condition that the maximal disks are tangent to two contour parts makes our skeleton insensitive to noise and contour deformations. The computation with particle filters assures that the skeleton paths are connected, vary smoothly, and are one pixel thick.

The final skeleton consists of the skeleton paths between all pairs of salient points. For a given set of salient contour points, we obtain an excellent skeleton without any pruning process. We use DCE to generate salient points, since it is proved in Bai *et al.*,[4] each DCE computed convex salient point is guaranteed to be a skeleton endpoint.

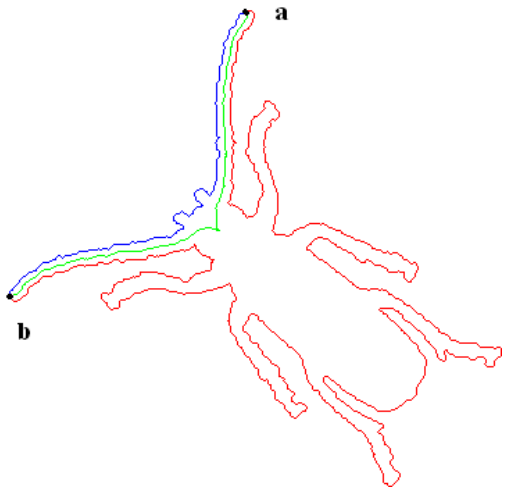

Fig. 3. In green a single skeleton path $p(a, b)$ from a to b computed by our algorithm. The salient points a and b divide the contour into two parts $C = C_1 \cup C_2$ marked with red and blue colors, respectively. $p(a, b)$ is composed of centers of maximal disks that are tangent both to C_1 and to C_2.

As in our case the target function is nonlinear, the Dynamic Programming (DP), which can only solve the linear function, will carry contour noise to the skeleton. Compared to DP, the particle filter can get rid of the noise and local solutions. It can allow branching and carrying multiple solutions. Therefore, we use a particle filter to find the skeleton path between any pair of the salient points instead of DP. Particle filters are also known as Sequential Monte-Carlo (SMC) methods, which have the ability to carry multiple hypotheses, and are widely used to track multiple targets with cluttered background in image sequences. The first application of particle filters in Computer Vision is in the tracking of object contours,[13,14] Tracking of tracking of motion boundaries is used for motion estimation in Ref. 7. The first application of particle filters to static images is presented in Ref. 25 where particle filters are applied to perform inference over a spatial chain of edge pixels rather than over a temporal chain. An extension of SMC that performs inferences on arbitrarily structured graphical models has been proposed in Refs. 15, 28 and applied to an edge linking task in Ref. 15.

The rest of the paper is organized as follows: our approach to computing skeleton paths is introduced in Sec. 2. The construction of the whole skeleton is presented in Sec. 3. The experimental results are shown in Sec. 4. Finally, the conclusion is presented in Sec. 6.

2. Computing Skeleton Paths with a Particle Filter

Let a and b be two convex, salient contour points. As stated in the introduction, we use DCE polygon simplification to compute the salient points, since all convex vertices of the DCE simplified polygon are guaranteed to be skeleton endpoints. The way to obtain the endpoints is not limited to using DCE, and there are some other

methods for computing the salient points on the contour that is fit for the proposed method, such as visual curvature.[18] Our goal is to obtain a skeleton path from a to b. We use $x^j_{1:t}$ to denote a sequence of skeleton points of particle j at time step t, i.e. $x^j_{1:t} = x^j_1, \ldots, x^j_t$. Then x^j_t is the current endpoint of the particle j at the step t. Let $N(x^j_t)$ represent the set of 8-nearest neighbors of all skeleton points of particle j.

We initialize with n particles, each equal to a, and the initial weights of the particles are $1/n$. At each iteration, we consider eight possible continuations of particle $x^j_{1:t-1}$ as the 8-nearest neighbors of x^j_{t-1}. (Here we benefit from the fact that a digital image is a discrete structure.) We obtain an eight extensions of particle $x^k_{1:t} = \{x^j_{1:t-1}, x^k_t\}$ for each of the eight neighbors $x^k_t \in N(x^j_{t-1})$. The index k of particle $x^k_{1:t}$ may be different from j, since particle j has eight extensions corresponding to the eight neighbors $N(x^j_{t-1})$ of x^j_{t-1}.

Now we derive a particle filter algorithm that is particularly suitable for computation in digital images. Our goal is to estimate the posterior $p(x_{1:t}|z_{1:t})$ over all potential skeleton paths in a given shape. Our observations $z_{1:t} = \{z_1, z_2, \ldots, z_t\}$ represent distances to the shape contour (a detailed definition follows below). Each particle represents a particular skeleton path. We will follow the framework of a particle filter algorithm called sampling importance resampling (SIR) filter,[10] which can be summarized as follows:

(1) *Prediction by Sampling*: The next generation of particles $\{x^k_{1:t}\}_k$ is obtained from the generation $\{x^j_{1:t}\}_{j-1}$ by sampling from a proposal distribution π (defined below).

We use prior boosting in prediction by sampling.[12] It allows us to capture multimodal likelihood regions in the posterior. In prior boosting we sample more than one follower for each particle so that different followers can capture different modes of the proposal. As described above, the fact that we work in digital images naturally suggests the eight followers be the eight neighbors of the latest pixel in each particle sequence. Thus, we increase the number of particles from N to 8N, which is then reduced back to N in the resampling step (3).

(2) *Importance Weighting*: An importance weight is assigned to each particle according to the importance sampling principle $w^k_t = \frac{p(x^k_{1:t}|z_{1:t})}{\pi(x^k_{1:t}|z_{1:t})}$. The weights account for the fact that the proposal distribution is usually not equal to the target distribution $p(x_{1:t}|z_{1:t})$.

(3) *Resampling*: Particles are drawn with replacement proportional to their importance weights. The weight of each of the eight new particles is defined as:

$$w^k_t = \frac{p(x^k_{1:t}|z_{1:t})}{\pi(x^k_{1:t}|z_{1:t})} = \frac{\eta p(z_t|x^k_{1:t}, z_{1:t-1}) p(x^k_t|x^j_{t-1})}{\pi(x_t|x^j_{1:t-1}, z_{1:t})} \frac{p(x^j_{1:t-1}|z_{1:t-1})}{\pi(x^j_{1:t-1}|z_{1:t-1})}$$

$$\propto \frac{p(z_t|x^k_t) p(x^k_t|x^j_{t-1})}{\pi(x_t|x^j_{1:t-1}, z_{1:t})} w^j_{t-1}, \tag{2}$$

where w^j_{t-1} is the weight of particle x^j_{t-1} and $\eta = 1/p(z_t|z_{1:t-1})$ is a normalization factor resulting from Bayes rule that is equal for all particles. Now we make an

important assumption that the proposal distribution $\pi(x_t|x^j_{1:t-1}, z_{1:t})$ is uniform. This is justified in our context by the fact that each point is a pixel that has eight neighbors, and continuation to each of the eight neighbors is equally probable. Therefore, we obtain

$$w^k_t \propto p(z_t|x^k_t)p(x^k_t|x^j_{t-1})w^j_{t-1} \tag{3}$$

The conditional probabilities in Eq. (3) are defined below based on digital topology of paths in digital images $p(x^k_t|x^j_{t-1})$ and on geometric properties of skeletons $p(z_t|x^k_t)$.

The conditional probability of the new particle $x^k_{1:t}$ generated by extending the jth particle is given by:

$$p(x^k_t|x^j_{1:t-1}) = \begin{cases} 1, & \text{if } x^k_t \in N(x^j_{t-1}) - N(x^j_{1:t-1}) \\ 0.01, & \text{else} \end{cases} \tag{4}$$

The main contribution of this probability is to avoid visiting the same pixels again, since we do not want the particle path to go backward, which would create a loop in the skeleton path or perturb it. Hence, we assign very low probability to the neighbors of x^j_{t-1} that already belong to the sequence of particle $x^j_{1:t-1}$.

In order to calculate $p(z_t|x^k_t)$, we recall that the contour is divided into two parts C_1 and C_2. Let d_1, d_2 represent the minimum distance from the point x^k_t to each of the parts, which for a correct skeleton paths both should be equal to the radius of the maximal disk centered at x^k_t. In particular, we should have $d_1 = d_2$. Thus, our observation z_t is composed of two distances d_1, d_2 from the contour parts C_1 and C_2. Figure 4 illustrates our computation of $p(z_t|x^k_t)$. Consider two different points P_1 and P_2 as candidates for the skeleton point x^k_t. It is obvious that P_1 is more likely to be the center of a maximal disk with respect to the contour parts C_1 and C_2 than P_2, since $D' = |d'_1 - d'_2|$ is smaller than $D = |d_1 - d_2|$.Therefore, we assume that the

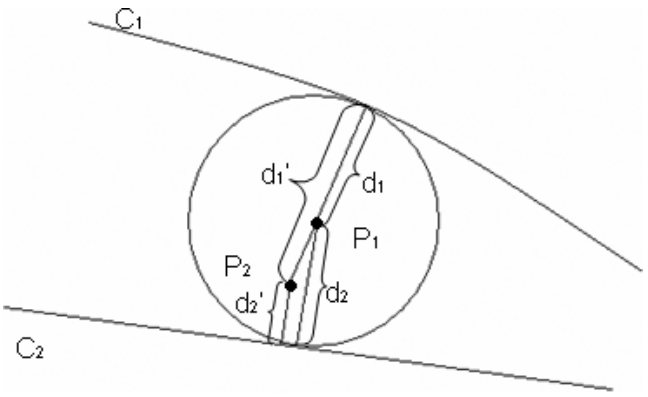

Fig. 4. Point P_1 is more likely to be a skeleton point than point P_2.

observation density is a Gaussian function of the difference $d_1 - d_2$:

$$p(z_t|x_t^k) = \frac{1}{\sqrt{2\pi}\sigma} e^{\frac{-(d_1-d_2)^2}{2\sigma^2}} \tag{5}$$

The outline of the derived particle filter algorithm is as follows:

From the "old" sample set $\{(x_{t-1}^j, w_{t-1}^j) : j = 1, \ldots, N\}$ at the time step $t-1$, construct a new sample set $\{(x_t^j, w_t^j) : j = 1, \ldots, N\}$ for step t.

For $j = 1$ to N iterate steps (1)−(3):

(1) **Prediction by Sampling**:
For each particle j, we extend it to eight particles by $x_{1:t}^k = \{x_{1:t-1}^j, x_t^k\}$, where $x_t^k \in N(x_{t-1}^j)$.

(2) **Importance Weighting**:
Compute the weights $w_t^k = p(z_t|x_t^k)p(x_t^k|x_{t-1}^j)w_{t-1}^j$ and normalize the weights so that $\sum_k w_t^k = 1$.

(3) **Subsampling**:
Draw N particles from the current set of $8N$ particles with probabilities proportional to their weights.

Finally, the particle with the highest weights is selected, which represents a skeleton path. There are two important differences in comparison to the standard sampling importance resampling (SIR) filter. First, our prediction by sampling considers all possible extensions to the eight neighbors , this is why our proposal distribution is uniform. Second, since our prediction by sampling increases the number of particles to $8N$, we replaced resampling with subsampling in order to reduce the number of particles to N. We modified the residual resampling to obtain the residual subsampling.

Figure 3 shows an example of one skeleton path generated by the above algorithm. The blue and red parts represent the two different parts C_1, C_2 of the contour separately, which are divided by the two vertices. The green line is the skeleton path generated by our algorithm. The skeleton path is in the middle of the two contour parts, which is the main property of an excellent skeleton. The skeleton path does not have any redundant branches and it is insensitive to boundary noise. These properties follow from the fact that the observation density $p(z_t|x_t^k)$ is computed with respect to the contour partitions C_1 and C_2 induced by two salient points. The conditional probability $p(x_t^k|x_{t-1}^j)$ is responsible for computing smooth paths that are one pixel thick. The statistical framework of particle filter assures that the local noise on pixel level does not distort the skeleton paths.

3. Combining Skeleton Paths to form a Complete Skeleton

The skeleton is the union of paths between all the endpoints. There are two steps to combine all the skeleton paths into one image. The first step is generating all the paths between all the endpoints based on the method introduced in Sec. 2.

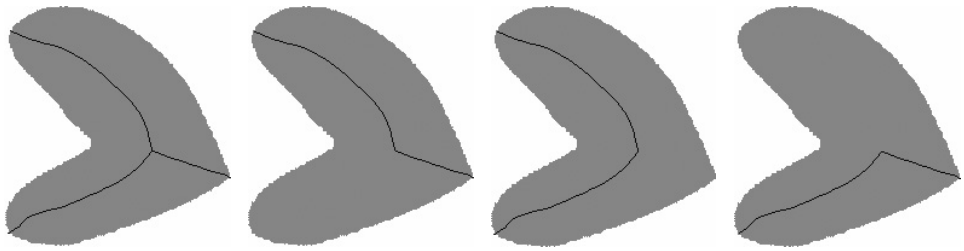

(a) (b) (c) (d)

Fig. 5. The skeleton in (a) is constructed by combining the paths in (b)−(d) together. These are all possible skeleton paths between the three DCE vertices, which are the skeleton endpoints.

The second step is combining all the paths together to obtain the skeleton. For example, the skeleton of the heart in Fig. 5(a) is the union of the skeleton path of Figs. 5(b)−5(d).

4. Experiments

In this section, we evaluate the proposed method in two parts: (1) we show that the skeleton is stable to the noise and deformation and (2) we compare it to other methods. Actually, in the field of computing skeleton, there is no quantitative way to define whether the results are good or not. If the skeleton can fit the six properties described in the introduction, the skeleton is good. From all of the results listed below, we can state that the proposed approach can generate excellent skeletons which satisfy the six properties. Besides, according to the comparison experiments, the proposed method can obtain much better skeleton than many other approaches.

4.1. *Test on noisy images*

The results in Fig. 6 show that the proposed method is insensitive to even substantial noise in contours. For each shape, there is one image without noise and one image with substantial noise. The similarity of the obtained skeletons illustrates the stability of the proposed method. In particular, there are no branches generated by the boundary noise, and the skeletons still preserve the topological and geometric structure of the objects. Other methods cannot obtain stable skeletons on noisy images. Most of them will have extra branches or distorted skeletons.

The extraordinary stability of our skeletons in the presence of large inner-class shape variations is demonstrated in Fig. 7.

Although the objects differ significantly from each other, the obtained pruned skeletons have the same global structure. Moreover, the thin tails of the camels remained in the skeleton, which cannot be achieved by most of the other pruning methods, since they may shorten or disconnect the skeleton. The final DCE simplified polygons are also shown overlaid on the shapes with red segments.

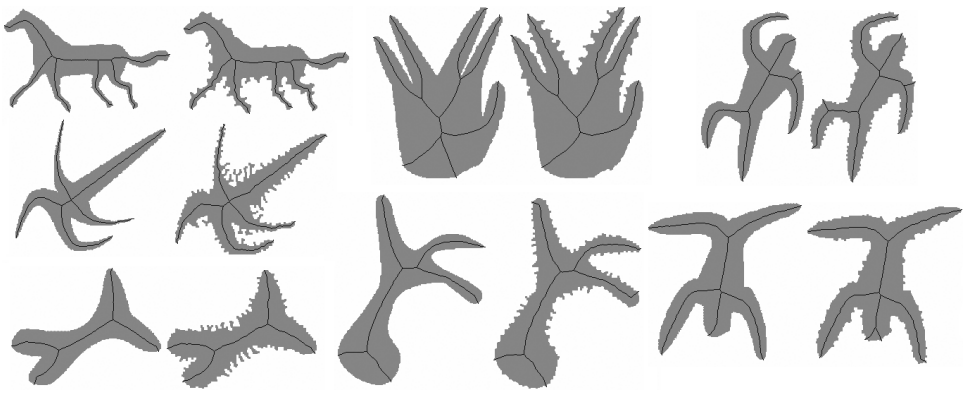

Fig. 6. For each shape, there is one image without noise and one image with substantial noise. The obtained skeletons are very similar.

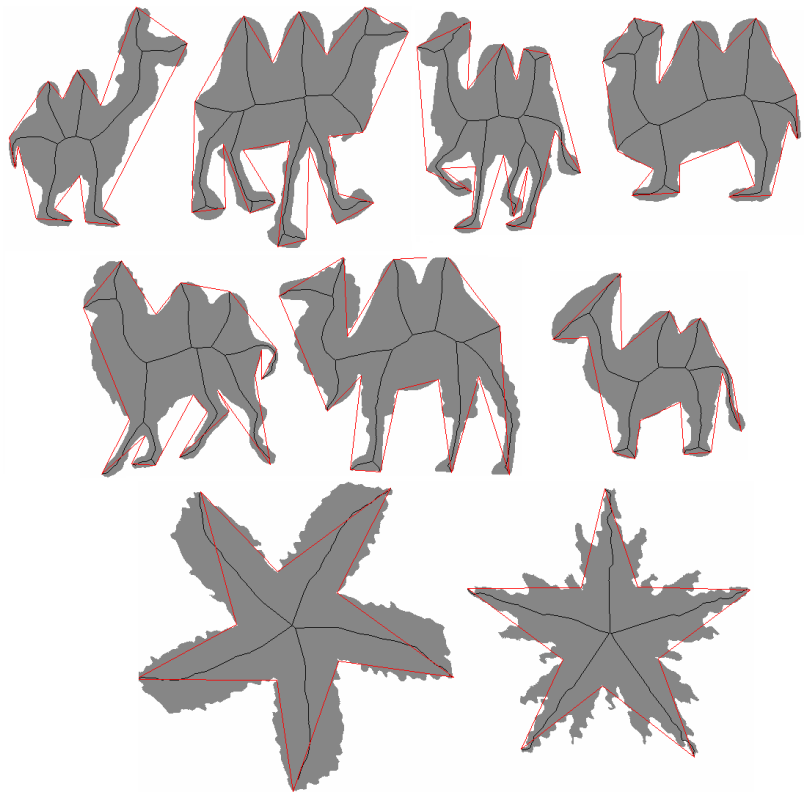

Fig. 7. The results on some shapes from the MPEG-7 database illustrate extraordinary stability of our skeletons in the presence of large shape variances. The red lines illustrate the DCE polygons.

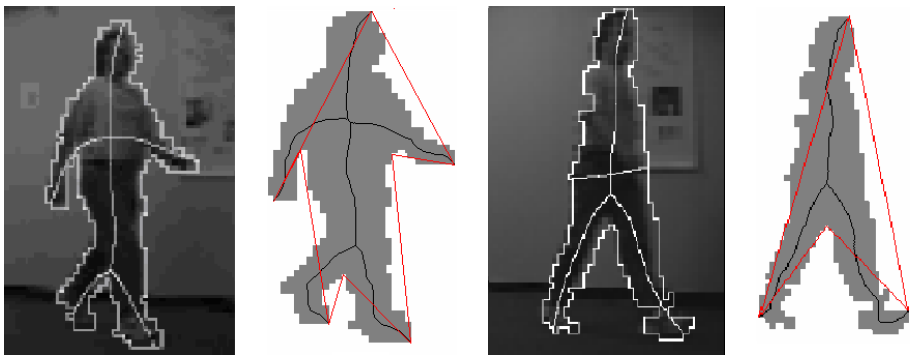

(a) (b) (c) (d)

Fig. 8. Comparison between (a) the fixed topology skeleton,[14] (c) and (b, d) our skeleton. The red lines illustrate the DCE polygons.

4.2. *Comparison to to other methods*

We compare our method to the fixed topology method,[11] which also starts with a small set of salient points. However, the fixed topology skeleton requires that the skeleton junction points are estimated. We do not need to estimate the junction points. Two example results of the fixed topology method[11] are shown in Figs. 8(a) and 8(c). As can be clearly seen, the obtained skeleton is not positioned accurately in that many skeleton points are not centers of maximal disks. In contrast, as shown in Figs. 8(b) and 8(d) all of our skeleton points are the centers of maximal disks, and therefore they are exactly symmetrical to the shape boundary. In addition, observe the presence of phantom horizontal skeleton branches in Fig. 8(c). They do not reflect any real structural information. Due to the stability of DCE, the proposed method does not introduce any phantom branches.

Figure 9 shows a comparison of our approach (b) with the method proposed by Ogniewicz and Kübler[24] (a), which has inaccurate, half-shortened branches that are not related to any obvious boundary features. Other experimental results of the proposed method prove that it is able to completely eliminate all the unimportant branches and still preserve the main structure. Our method does not suffer from the shortening of main skeleton branches and it preserves the topology of the skeleton. Moreover, the obtained skeletons seem to be in accordance with human perception, as it satisfies the six properties of the skeleton.

The method introduced by Bai *et al.*[4] can obtain excellent skeletons which contain most of the properties of ideal skeletons, but it cannot guarantee that the skeleton is one-pixel wide, which is illustrated in Fig. 10(a). As shown in Fig. 10(b), our method produces one-pixel wide skeletons.

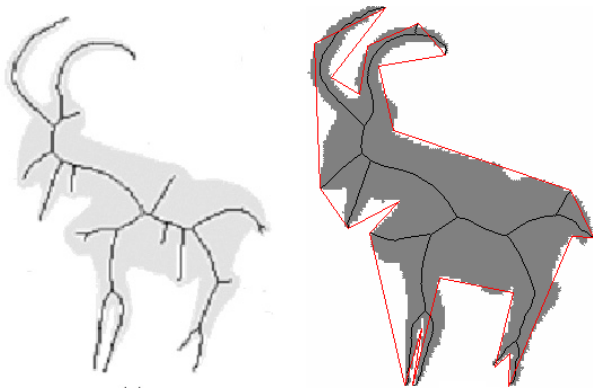

(a) (b)

Fig. 9. Comparison between pruning result in Ref. 24 in (a) and our results in (b).

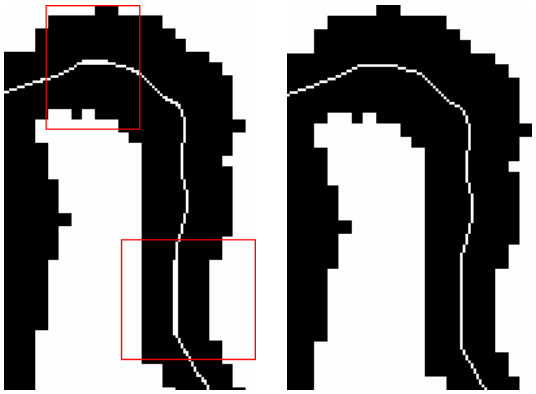

(a) (b)

Fig. 10. Comparison between pruning result in Ref. 4 in (a) and our results in (b).

5. Extension to Gray Images

In this section, we show that our method has a potential to be extended to gray-scale images. For skeletonization for gray images, the major difficulty is to obtain the object's boundary. We applied our framework on top of the Skeleton Strength Map (SSM) computed by the approaches.[19,20] SSM is calculated from Euclidean distance transform of the edge maps, which can be considered as probabilistic map for the skeleton points. The value at each pixel of SSM denote the confidence to be a skeleton point. Different from skeletonization for binary images, here we use the values of SSM as the observation density $p(z_t|x_t^k)$ in Eq. (5). Using strength maps for particle filters is not new, as it has been successfully applied in contour tracing.[23,25] Figure 11 shows a few example results by our methods. The endpoints for skeletal paths are selected manually, as the complete boundary cannot often be obtained from clutter

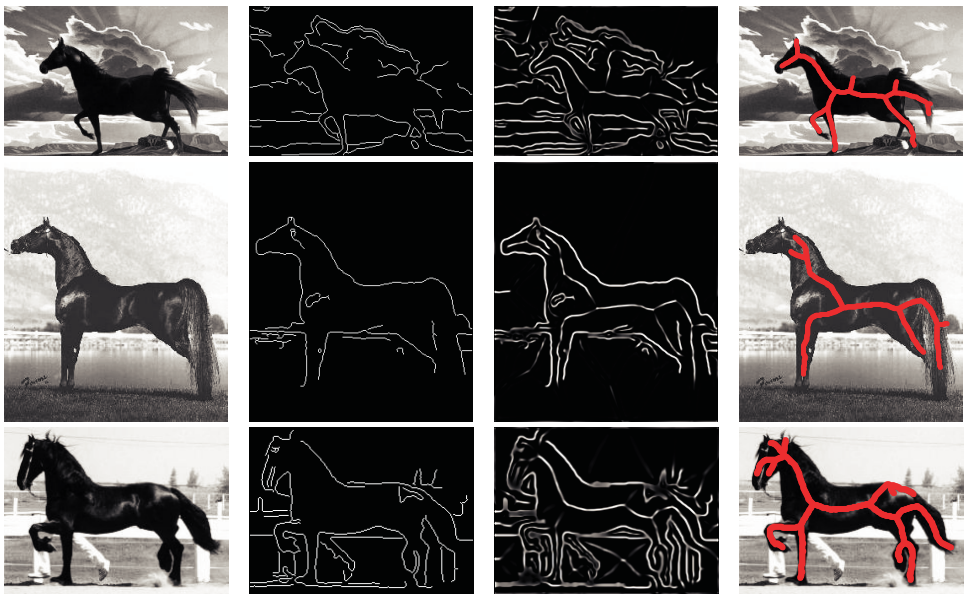

(a) (b) (c) (d)

Fig. 11. The results on gray images. (a) the original gray images, (b) the edge maps, (c) the SSMs based on (b), and (d) the results.

images. However, our experimental results still make sense, since manual initialization for contour grouping or segmentation has been widely used.[1,25,23]

6. Conclusion

In this paper, we establish a novel framework for skeleton computation that combines the geometric method of Discrete Curve Evolution with the statistical method of particle filters. The obtained skeletons do not have redundant skeleton branches and retain all the necessary visual branches. The experimental results demonstrate high stability of the obtained skeletons even for objects with extremely noisy contours, which is the key property required to measure the shape similarity of objects using their skeletons. Moreover, this method can guarantee the skeleton is one-pixel wide. The proposed particle filter framework easily extends to computing skeletons of gray level images when applied to SSM.

In future, we will extend the proposed approach to generate the skeleton for the shape with holes and 3D shapes, as the particle filter can deal with the condition that the path between two endpoints is not unique.

Acknowledgements

This work is supported in part by the National Natural Science Foundation of China No. 60903096.

References

1. N. Adluru, L. J. Latecki, R. Lakaemper, T. Young, X. Bai and A. Gross, Contour grouping based on local symmetry, *11th IEEE Int. Conf. Computer Vision (ICCV)* (2007).
2. S. Arulampalam, S. Maskell, N. Gordon and T. Clapp, A tutorial on particle filters for on-line non-linear/non-Gaussian Bayesian tracking, *IEEE Trans. Signal Processing* **50**(2) (2002) 174–188.
3. C. Aslan, A. Erdem, E. Erdem and S. Tari, Disconnected skeleton: Shape at its absolute scale, *IEEE Trans. Patt. Anal. Mach. Intell.* **30**(12) (2008) 2188–2201.
4. X. Bai, L. J. Latecki and W. Y. Liu, Skeleton pruning by contour partitioning with discrete curve evolution, *IEEE Trans. Patt. Anal. Mach. Intell.* **29**(3) (2007) 449–462.
5. X. Bai and L. J. Latecki, Path similarity skeleton graph matching, *IEEE Trans. Pattern Anal. Mach. Intell.* **30**(7) (2008) 1282–1292.
6. X. Bai, X. Yang, D. Yu and L. J. Latecki, Skeleton-based shape classification using path similarity, *Int. J. Patt. Recogn. Artif. Intell.* **22**(4) (2008) 733–746.
7. M. J. Black and D. J. Fleet, Probabilistic detection and tracking of motion boundaries, *Int. J. Comput. Vis.* **38**(3) (2003) 231–245.
8. H. Blum, Biological shape and visual science (Part I), *J. Theoret. Biol.* **38** (1973) 205–287.
9. W.-P. Choi, K.-M. Lam and W.-C. Siu, Extraction of the Euclidean skeleton based on a connectivity criterion, *Patt. Recogn.* **36** (2003) 721–729.
10. A. Doucet, N. de Freitas and N. Gordon (eds.), *Sequential Monte Carlo Methods in Practice* (Springer-Verlag, New York, 2001).
11. P. Golland and E. Grimson, Fixed topology skeletons, in *CVPR* (2000), pp. 10–17.
12. N. J. Gordon, D. J. Salmond and A. F. M. Smith, Novel approach to nonlinear/non-Gaussian Bayesian state estimation, *IEE Proc. F* **140**(2) (1993) 107–113.
13. M. Isard and A. Blake, Contour tracking by stochastic propagation of conditional density, *Proc. ECCV* (1998), pp. 343–356.
14. M. Isard and A. Blake, Condensation — conditional density propagation for visual tracking, *Int. J. Comput. Vis.* **29**(1) (1998) 5–28.
15. M. Isard, Pampas, Real-valued graphical models for computer vision, in *Proc. CVPR* (2003), pp. 613–620.
16. L. J. Latecki and R. Lakämper, Shape similarity measure based on correspondence of visual parts, *IEEE Trans. Patt. Anal. Mach. Intell.* **22**(10) (2000) 1185–1190.
17. L. J. Latecki and R. Lakämper, Polygon evolution by vertex deletion, *Proc. Int. Conf. Scale-Space* (1999), volume LNCS 1682.
18. H. Liu, L. J. Latecki and W.-Y. Liu, A unified curvature definition for regular, polygonal and digital planar curves, *Int. J. Comput. Vis.* **80**(1) (2008) 104–124.
19. L. J. Latecki, Q. Li, X. Bai and W. Y. Liu, Skeletonization using SSM of the distance transform, *ICIP* (2007), pp. 349–352.
20. Q. Li, X. Bai and W. Y. Liu, Skeletonization of gray-scale image from incomplete boundaries, *ICIP* (2008), pp. 877–880.
21. F. F. Leymarie and M. D. Levine, Simulating the grassfire transform using an active contour model, *IEEE Trans. Patt. Anal. Mach. Intell.* **14**(1) (1992) 56–75.
22. J. S. Liu, R. Chen and W. H. Wong, Rejection control and sequential importance sampling, *J. Amer. Statist. Assoc.* **93**(443) (1998) 1022–1031.
23. C.-E. Lu, L. J. Latecki, G.-X. Zhu, Contour extraction using particle filters, in *ISVC* (2008), Vol. 2, pp. 192–201.
24. R. L. Ogniewicz, O. Kübler, Hierarchic Voronoi skeletons, *Patt. Recogn.* **28**(3) (1995) 343–359.

25. P. Pérez, A. Blake and M. Gangnet, Jetstream: Probabilistic contour extraction with particles, *Proc. Int. Conf. Computer Vision* (2001), pp. 524−531.
26. D. Shaked and A. M. Bruckstein, Pruning medial axes, *Comput. Vis. Imag. Underst.* **69** (2) (1998) 156−169.
27. K. Siddiqi, A. Shkoufandeh, S. Dickinson and S. Zucker, Shock graphs and shape matching, *ICCV* (1998), pp. 222−229.
28. E. B. Sudderth, A. T. Ihler, W. T. Freeman and A. S. Willsky, Nonparametric belief propagation, in *Proc. CVPR* (2003), Vol. 1, pp. 605−612.
29. X. You, Q. Chen, B. Fang and Y. Y. Tang, Thinning character using modulus minima of wavelet transform, *Int. J. Patt. Recogn. Artif. Intell.* **20**(1) (2006) 361−376.
30. S. C. Zhu and A. Yuille, FORMS: A flexible object recognition and modeling system, *ICCV*, 1995.

Yuchun Tang is a lecture of Shandong University School of Medicine. In 2009, he received PhD in Human Anatomy, Histology and Embryology from Shandong University. From April 2008 to April 2009, he was a visiting scientist at Lab of Neuro Imaging, UCLA.

Xiang Bai received BS in electronics and information engineering from Huazhong University of Science and Technology (HUST), Wuhan, China, in 2003 and MS in electronics and information engineering from HUST in 2005. In 2009, he received his PhD degree in Communication and Information Engineering from HUST. From Jan. 2006 to May 2007, he worked in Department of Computer Science and Information of Temple University. From Oct. 2007 to Oct. 2008, he studied in the Department of Neurology of University of California, Los Angeles as a joint PhD student. Currently, he has joined the EI Department of HUST as a faculty member. His research interests include computer graphics, computer vision and pattern recognition.

Xingwei Yang received his B.E. degree in Electronics and Information Engineering from Huazhong University of Science and Technology (HUST), Wuhan, China, in 2002. Now, he is a Ph.D. candidate in the department of Computer and Information Science at Temple University.

Liang Lin received the BS and PhD degrees from Beijing Institute of Technology (BIT) in 1999 and 2008, respectively. He studied in the Department of Statistics at the University of California, Los Angeles (UCLA), as a visiting PhD student during 2006-2007. He was a postdoctoral research fellow at the Center for Image and Vision Science (CIVS) at UCLA, and a research scientist at Lotus Hill Institute (www.lotushill.org) during 2007 2009. He is now an associate professor at Sun Yat-Sen University (SYSU) and the deputy director of Lab of Intelligent Information Processing at SYSU. His research interests include but are not limited to object recognition, graph and shape matching, image parsing, and visual tracking.

Shuwei Liu is a professor of department of Human Anatomy and Embryology, Shandong University and Vice-Dean of Shandong University School of Medicine. He also serves as an Executive Vice-Dean of Shandong University Graduate School.

Longin Jan Latecki received the PhD degree in computer science from Hamburg University, Germany, in 1992. He is an associate professor of computer science at Temple University, Philadelphia. His main research interests include shape representation and similarity, object detection and recognition in images, robot perception, data mining, and digital geometry. He has published over 175 research papers and books. He is an editorial board member of Pattern Recognition and International Journal of Mathematical Imaging. He received the Pattern Recognition Society Award together with Azriel Rosenfeld for the best article published in Pattern Recognition in 1998. He is the recipient of the 2000 Olympus Prize, the main annual award, from the German Society for Pattern Recognition (DAGM).